ISSN 1028-334X, Doklady Earth Sciences, 2006, Vol. 406, No. 1, pp. 89–93. © Pleiades Publishing, Inc., 2006.
Original Russian Text © I.V. Anisimova, A.B. Kotov, V.A. Glebovitsky, E.B. Sal'nikova, S.Z. Yakovleva, S.D. Velikoslavinsky, N.Yu. Zagornaya, 2006, published in Doklady Akademii Nauk, 2006, Vol. 406, No. 3, pp. 355–360.

GEOCHEMISTRY

Age Limits and Formation Duration of Paleoproterozoic Volcanic Belts in the Central Aldan Shield

I. V. Anisimova, A. B. Kotov, Corresponding Member of the RAS V. A. Glebovitsky, E. B. Sal'nikova, S. Z. Yakovleva, S. D. Velikoslavinsky, and N. Yu. Zagornaya

Received July 29, 2005

DOI: 10.1134/S1028334X06010223

The available geological, geochronological, geochemical, and isotopic data furnish evidence that the Paleoproterozoic protoliths of metavolcanic rocks in the central Aldan Shield were formed within a geodynamic system of the active continental margin of the Olekma–Aldan microplate and the Fedorovka island arc [1–3] as a result of the deposition of volcanosedimentary rocks in the Balaganakh greenstone belt (active continental margin) along with the formation of the Fedorovka volcanic sequence and the protoliths of the associated orthogneisses of the Timpton Complex. The evolution of this system was completed by the collision of the Fedorovka island arc and the Olekma–Aldan continental microplate and the development of the deep-seated thrust faults of the Chuga and Fedorovka systems ~1992 Ma ago [1, 4]. It has been established that the protoliths of metavolcanic rocks of the Fedorovka Sequence have an age of 2006 ± 3 Ma [3], while the protoliths of orthogneisses of the Timpton Complex are dated back to 2011 ± 2 Ma [4]. A reliable age for the Balaganakh greenstone belt was unknown until recently. It was only supposed that its age falls within a range of 2.0–2.3 Ga [1, 2, 5]. This estimate did not allow for a specification of the origination of the volcanic belt at the margin of the Olekma–Aldan continental microplate or for an assessment of the life period of the geodynamic system under consideration. This, in turn, hampered the elaboration of integrated geodynamic models of the Precambrian complexes in the Aldan Shield.

To solve this problem, we carried out the U–Pb geochronological study of metavolcanic rocks from the Balaganakh greenstone belt, which is localized in the eastern part of the junction of the Chara–Olekma and Aldan geoblocks of the Aldan Shield (Fig. 1). This belt includes numerous tectonic fragments (Balaganakh, Sogalokh, Kaverdag, Nirelyakh, and Imenkakh) composed of diverse metasedimentary and metavolcanic rocks of the Balaganakh Sequence that are confined to the Aldan–Kilier Fault Zone (Fig. 1). The Balaganakh tectonic fragment located at the northern flank of the eponymous greenstone belt has been the best studied to date. This fragment, 10×3 km^2 in area, is composed of amphibole and biotite–amphibole schists (basalts, andesites, and dacites or graywackes), biotite microgneisses (dacites), mica and two-mica schists, and gneisses (mudstones) of the amphibolite-facies metamorphism.

The biotite–amphibole schists have been chosen as objects of the U–Pb geochronological study. Judging from their chemical composition, andesites and dacites or graywackes of the first cycle of erosion of these volcanic rocks served as protoliths. The location of samples is shown in Fig. 1, and the results obtained are summarized in the table and in Figs. 2 and 3.

Metaandesites. Zircons separated from metaandesite (sample 201b) of the Balaganakh fragment are represented by subhedral, transparent, and less frequent turbid pale pink or pink short- and long-prismatic crystals, the subisometric form of which is related to the amphibolite-facies recrystallization. The crystals have prismatic {100} and {110} and dipyramidal {101} faces (Fig. 2a). One can see the shaded areas at crystal margins and the distinct primary magmatic zoning in transmitted light. Cathode luminescence analysis reveals the zonal structure of zircon crystals. In general, the zircon grains are characterized by a lower luminescence and the sporadic presence of relict cores (Fig. 2b). Local zones of high luminescence at the margins of some grains are related to the partial high-temperature recrystallization of zircon (Fig. 2b). The size of zircon grains varies from 50 to 150 μm (K_{elong} = 1.0–3.0).

Figure 3 shows three points of isotopic compositions of zircon microsamples (3–5 grains) subjected to preliminary air abrasion (table, nos. 2, 4, 5). They define a regression line, the upper intercept of which with concordia corresponds to an age of 2051 ± 28 Ma, while the lower intercept yields 133 ± 180 Ma

Institute of Precambrian Geology and Geochronology, Russian Academy of Sciences, nab. Makarova 2, St. Petersburg, 199034 Russia;
e-mail: conan@ik4843.spb.edu

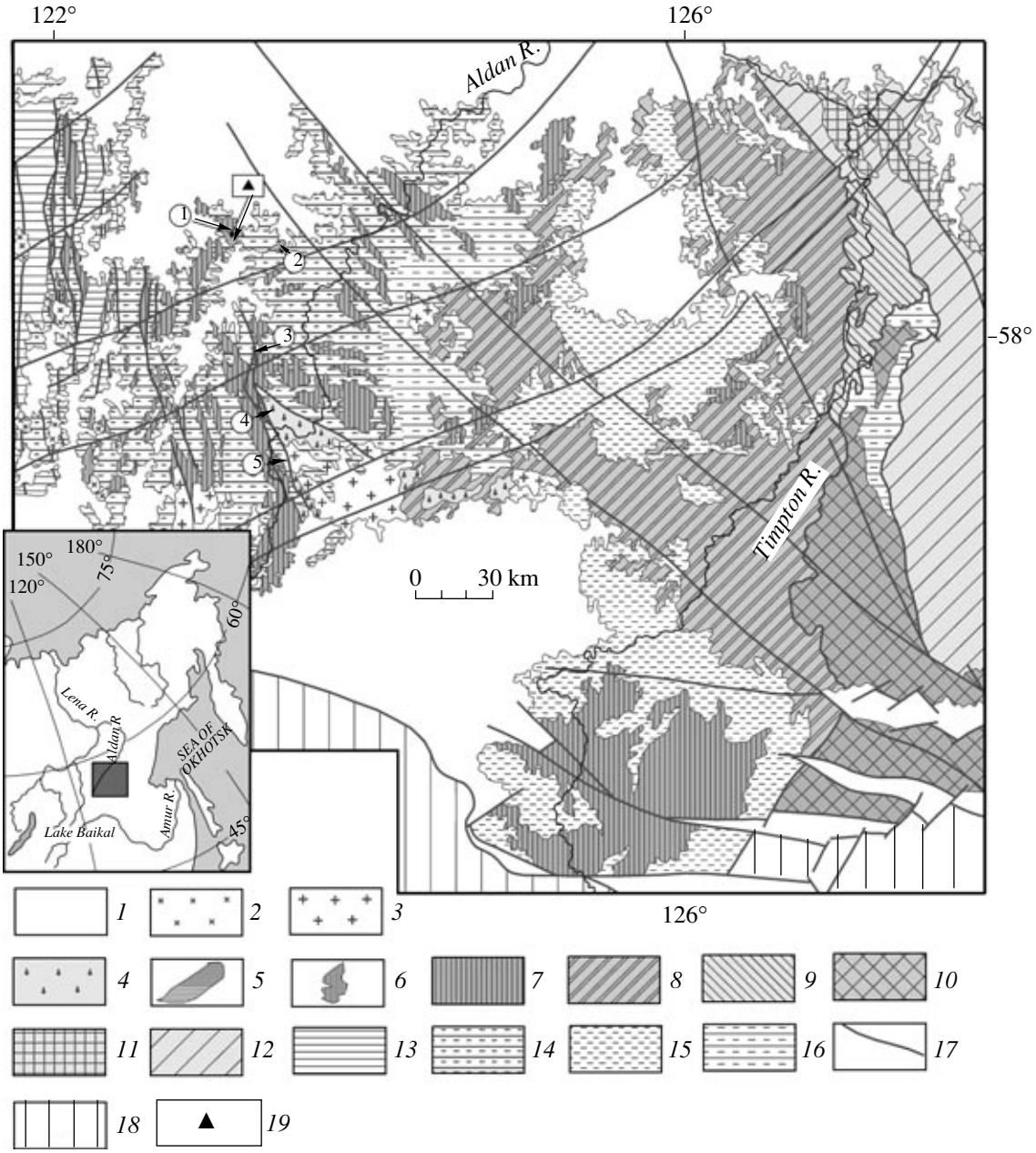

Fig. 1. Schematic geological map of the central Aldan Shield (Timpton–Aldan interfluve). (*1*) Quaternary, Mesozoic, Paleozoic, and Neoproterozoic platform cover; (*2*) unspecified Paleoproterozoic granitoids; (*3*) granitoids of the Dzhaltunda Complex; (*4*) igneous rocks of the Ungra Complex; (*5*) volcanosedimentary rocks of the Balaganakh greenstone belt; (*6*) metasedimentary and metavolcanic rocks of the Subgan Complex; (*7–12*) high-grade metasedimentary and metavolcanic rocks of the Aldan granulite–gneiss complex: (*7*) unspecified Kurumkan, Amedichi, and Chuga sequences (mainly garnet–cordierite–biotite, garnet–sillimanite–cordierite–biotite, sillimanite–biotite, and cordierite–sillimanite–biotite gneisses; quartzites; two-pyroxene–hornblende and diopside–hornblende crystalline schists); (*8*) Fedorovka Sequence (hypersthene–biotite, hypersthene–biotite–hornblende, and diopside–hornblende plagiogneisses; two-pyroxene–hornblende, diopside–hornblende, and hornblende crystalline schists; rare calciphyre interlayers); (*9*) Idzha Sequence (hypersthene, hypersthene–diopside, and hypersthene–diopside–hornblende plagiogneisses with interlayers and lenses of hypersthene–diopside and hypersthene–diopside–hornblende crystalline schists; diopside–scapolite and diopside–plagioclase schists with thin interlayers of garnet–biotite and garnet–hypersthene–biotite gneisses); (*10*) Seim Sequence (garnet–biotite gneisses and plagiogneisses; high-Al sillimanite–cordierite–garnet gneisses; two-pyroxene and diopside–hornblende plagiogneisses; quartzites; sporadic interlayers of calc–silicate rocks); (*11*) Kyurikan Sequence (rhythmic intercalation of garnet–biotite, hypersthene–biotite, biotite, hypersthene–diopside, and hypersthene–diopside–hornblende plagiogneisses; marbles and calciphyres; diopside and diopside–hornblende crystalline schists); (*12*) Kholbolokh Sequence (garnet–biotite plagiogneisses with sporadic interlayers of calc-silicate rocks; hypersthene, diopside, and two-pyroxene plagiogneisses with interlayers of basic crystalline schists); (*13–15*) granite gneisses of (*13*) Olekma, (*14*) Timpton, and (*15*) Aldan complexes; (*16*) unspecified granite gneisses of the Aldan and Timpton complexes; (*17*) faults; (*18*) conjugation of the Aldan Shield and Dzhugdzhus–Stanovoi fold zone; (*19*) location of samples for geochronological study. Tectonic fragments of the Balaganakh greenstone belt (numerals in circles): (1) Balaganakh, (2) Sogalokh, (3) Kaverdag, (4) Nirelyakh, (5) Imenkakh.

Results of U–Pb isotopic study of single zircon grains from amphibole schists of the Balaganakh greenstone belt

Nos.	Size, μm and characteristics of grains	U/Pb[a]	Isotopic ratios corrected for procedure blank and common lead			
			$^{206}Pb/^{204}Pb$	$^{207}Pb/^{206}Pb$	$^{208}Pb/^{206}Pb$	$^{207}Pb/^{235}U$
Sample 201b (andesite)						
1	50–100, A = 35%, 1 grain	2.52	794	0.1230 ± 8	0.1433 ± 1	5.691 ± 48
2	50–100, A = 35%, 5 grains	2.23	304	0.1263 ± 13	0.1226 ± 1	5.053 ± 87
3	50–100, A = 30%, 1 grain	3.14	335	0.1007 ± 4	0.1984 ± 1	3.405 ± 20
4	50–100, A = 25%, 2 grains	3.52	1575	0.1283 ± 2	0.0941 ± 1	4.757 ± 26
5	50–100, A = 25%, 5 grains	2.15	167	0.1277 ± 10	0.1922 ± 2	5.427 ± 86
Sample AI-6 (dacite)						
6	>100, Insoluble fraction retained after 2 h	2.06	194	0.1273 ± 11	0.3056 ± 1	6.056 ± 56
7	>100, A = 20%, 14 grains	2.75	457	0.1270 ± 8	0.2230 ± 2	5.184 ± 34
8	>100, A = 30%, 10 grains	3.09	777	0.1275 ± 5	0.1915 ± 1	4.853 ± 23

Nos.	Size, μm and characteristics of grains	Isotopic ratios corrected for procedure blank and common lead	*Rho*[·]	Age, Ma		
		$^{206}Pb/^{238}U$		$^{207}Pb/^{235}U$	$^{206}Pb/^{238}U$	$^{207}Pb/^{206}Pb$
Sample 201b (andesite)						
1	50–100, A = 35%, 1 grain	0.3356 ± 26	0.72	1930 ± 16	1865 ± 15	2000 ± 12
2	50–100, A = 35%, 5 grains	0.2887 ± 19	0.56	1831 ± 23	1647 ± 20	2047 ± 21
3	50–100, A = 30%, 1 grain	0.2453 ± 11	0.67	1506 ± 9	1414 ± 7	1636 ± 7
4	50–100, A = 25%, 2 grains	0.2691 ± 14	0.95	1777 ± 10	1536 ± 8	2074 ± 4
5	50–100, A = 25%, 5 grains	0.3047 ± 47	0.88	1888 ± 30	1729 ± 27	2066 ± 6
Sample AI-6 (dacite)						
6	>100, Insoluble fraction retained after 2 h	0.3451 ± 27	0.49	1984 ± 18	1911 ± 15	2060 ± 18
7	>100, A = 20%, 14 grains	0.2690 ± 18	0.48	1850 ± 12	1972 ± 10	2057 ± 13
8	>100, A = 30%, 10 grains	0.2756 ± 12	0.66	1974 ± 9	1569 ± 7	2066 ± 8

Note: (a) Weight of zircon grain was not determined; U/Pb ratio was determined for a conditional charge; (b) correlation coefficient of $^{207}Pb/^{235}U$ and $^{206}Pb/^{238}U$ errors. (A-20%) Percentage of the material removed during the air abrasion of zircon [8]. Uncertainties (2σ) correspond to the last significant digits. Accessory zircons were separated with the standard techniques using heavy liquids. The zircon crystals selected for the U–Pb geochronological study were subjected to the multistep removal of surficial impurities in alcohol, acetone, and 1 M HNO_3. Zircon grain or its fragment was washed with special pure water after each step. The breakdown of zircon and chemical separation of Pb and U were carried out following the modified technique of Krogh [9]. The procedure blank during measurements was <15 pg for Pb. The Pb and U isotopic compositions were measured on a Finnigan MAT-261 mass spectrometer with an electron multiplier (discrimination coefficient for Pb is 0.32 ± 0.11 amu). The experimental data were processed with the PbDat [10] and ISOPLOT [11] programs. The age was calculated using the commonly accepted constants of uranium decay [12]. Corrections for common lead were introduced in line with model values [13]. All uncertainties are given at the 2σ level.

(MSWD = 0.9). Data points of isotopic composition of the single zircon grains also subjected to air abrasion (table, points 1, 3) are located on the left side of discordia, most likely, owing to the incomplete removal of recrystallized zones.

Metadacites. Zircons from metadacite (sample AI-6) are represented by subhedral turbid, occasionally transparent, short- and less frequent long-prismatic pale pink crystals of rounded habit. The crystals have prismatic {100} and {110} and dipyramidal {101} faces (Fig. 2a). The crystal surfaces are corroded. The distinct zoning is observed in transmitted light. In general, the crystals are characterized by a lower birefringence and weak luminescence. The zonal structure is also detected in the regime of cathode luminescence. Some grains include recrystallized sectors in central zones with a higher luminescence (Fig. 2b). The zircon grains vary from 80 to 250 μm in size (K_{elong} = 1.0–3.0).

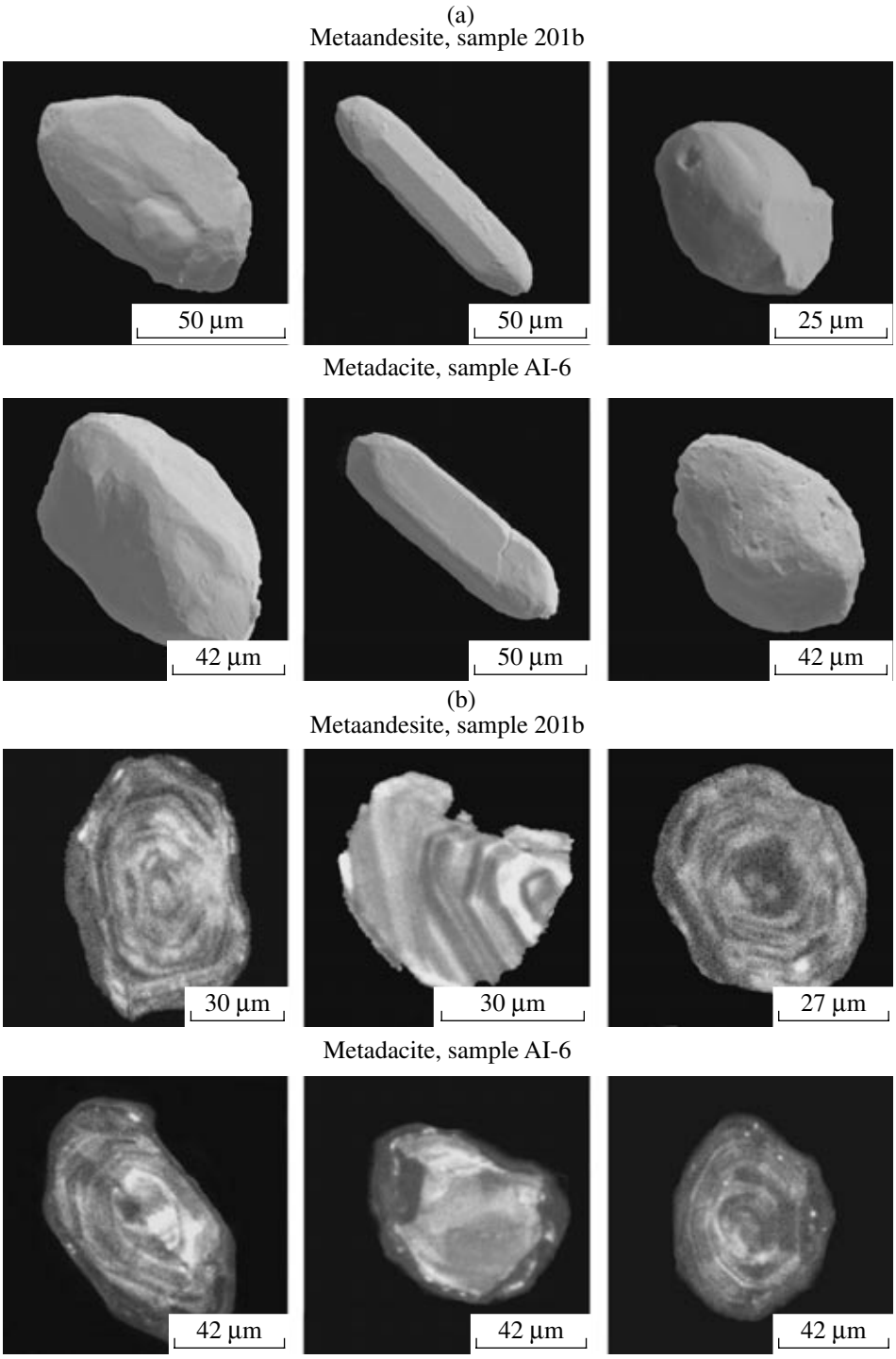

Fig. 2. Photomicrographs of zircon grains from amphibole schists of the Balaganakh greenstone belt obtained with an ABT-55 SEM (accelerating voltage is 25 kV): (a) SE, (b) CL with mini-CL cathode luminescent detector.

Two zircon microsamples (table, nos. 7, 8; 10 and 14 grains, respectively) subjected to air abrasion, as well as a residue after the acid treatment [6] of 14 grains during 2 h (table, no. 6), were used for geochronological study. Data points of these zircon fractions are arranged along discordia. The upper intercept with concordia corresponds to an age of 2055 ± 18 Ma and the lower intercept yields 61 ± 130 Ma (MSWD = 1.12) (Fig. 3).

The morphology and internal structure of zircon grains from metaandesites and metadacites of the Balaganakh greenstone belt testify to their magmatic origin.

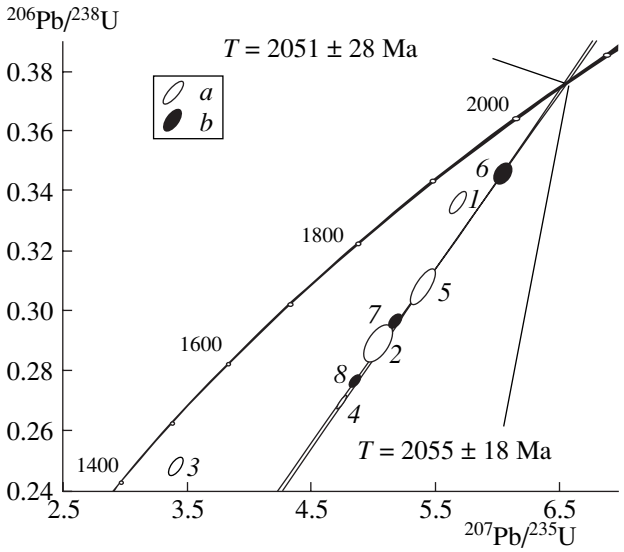

Fig. 3. Diagram with concordia for zircons from amphibole schists of the Balaganakh greenstone belt. Point numbers correspond to ordinal numbers in the table. (*a*) Metaandesite, sample 201b; (*b*) metadacite, sample AI-6.

Hence the obtained estimates of 2055 ± 18 and 2051 ± 28 Ma may be regarded as the age of crystallization of the initial melts.

The new results together with previous geochronological, geochemical, and isotopic data on the reference volcanic and plutonic complexes in the central Aldan Shield suggest the following scenario of the evolution of the geodynamic system of the active continental margin of the Olekma–Aldan microplate and the Fedorovka island arc.

2055 ± 18 Ma. The origination of the volcanic arc at the eastern (in present-day coordinates) margin of the Olekma–Aldan continental microplate. The onset of deposition of volcanosedimentary sequences in the Balaganakh greenstone belt.

2011 ± 2–2006 ± 3 Ma. The origination of the Fedorovka island arc. The accumulation of volcanics of the Fedorovka Sequence and the formation of protoliths of tonalite–trondhjemite orthogneisses of the Timpton Complex.

1993 ± 1. The formation of the Chuga and Fedorovka thrust systems due to the collision of the Fedorovka island arc and the Olekma–Aldan continental microplate [1, 4].

According to this scenario, the duration of the development of this geodynamic system was not longer than 80 Ma, and the life period of the Fedorovka island arc was only ~20 Ma. Thus, we have obtained a new piece of evidence in favor of the idea of relatively fast tectonic processes in the early Precambrian [7].

ACKNOWLEDGMENTS

We thank Yu.V. Plotkina and M.D. Tolkachev (Institute of Precambrian Geology and Geochronology) for the microscopic (SE, BSE, and CL) examination of zircons. This work was supported by the Russian Foundation for Basic Research (project no. 04-05-64810), the Foundation of the President of the Russian Federation for the Support of Leading Scientific Schools (grant no. NSh-615.2003.05), the Program of Fundamental Investigations of the Division of Earth Sciences, Russian Academy of Sciences *Isotope Geology: Geochronology and Sources of Matter*, and the Russian Science Support Foundation.

REFERENCES

1. A. B. Kotov, Doctoral Dissertation in Geology and Mineralogy (St. Petersburg, 2003).
2. I. V. Anisimova, A. B. Kotov, V. P. Kovach, *et al.*, in *Evolution of Tectonic Processes in the Earth's History* (Novosibirsk, 2004), pp. 6–7 [in Russian].
3. S. D. Velikoslavinsky, A. B. Kotov, E. B. Sal'nikova, *et al.*, Dokl. Akad. Nauk **393**, 91 (2004) [Dokl. Earth Sci. **393**, 1151 (2004)].
4. A. B. Kotov, V. P. Kovach, E. B. Sal'nikova, *et al.*, Petrologiya **347** (2), 236 (1995).
5. A. B. Kotov, I. V. Anisimova, V. A. Glebovitsky, *et al.*, Dokl. Akad. Nauk **398**, 661 (2004) [Dokl. Earth Sci. **399**, 1060 (2004)].
6. J. M. Mattinson, Contrib. Mineral. Petrol. **116**, 117 (1994).
7. K. C. Condie, *Plate Tectonics and Crustal Evolution* (Heinemann, Butterworth, New Mexico, 1997).
8. T. E. Krogh, Geochim. Cosmochim. Acta **46**, 637 (1982).
9. T. E. Krogh, Geochim. Cosmochim. Acta **37**, 485 (1973).
10. K. R. Ludwig, US Geol. Surv. Open-File Rept., No. 88-542 (1991).
11. K. R. Ludwig, *User's Manual for Isoplot/Ex, Version 2.10. A Geochronological Toolkit for Microsoft Excel* (Berkeley Geochronol. Center Spec. Publ., 1999), No. 1a.
12. R. H. Steiger, Earth Planet. Sci. Lett. **36** (2), 359 (1976).
13. J.S. Stacey and I. D. Kramers, Earth Planet. Sci. Lett. **26** (2), 207 (1975).